Applied Surface Science 62 (1992) 13–20
North-Holland

applied
surface science

Interaction between plasma sprayed YBaCuO and nimonic substrates

W. Lisowski [a,1], H. Hemmes [a], D. Jäger [b], D. Stöver [b] and A. van Silfhout [a]

[a] *Department of Applied Physics, University of Twente, P.O. Box 217, NL-7500 AE Enschede, The Netherlands*
[b] *Institut für Angewandte Werkstofforschung, Forschungszentrum Jülich, Postfach 1913, D-5170 Jülich, Germany*

Received 9 March 1992; accepted for publication 31 May 1992

The interaction of YBaCuO layers, deposited by atmospheric plasma spraying, with nimonic substrates at high temperature has been studied using X-ray photoelectron spectroscopy and Auger electron spectroscopy (AES). Both the region at the YBaCuO/nimonic interface and the surface of clean nimonic substrates after annealing in vacuum and oxygen have been studied in terms of chemical composition and peak shapes. Chromium was detected more than 20 μm deep in the YBaCuO layer. This is explained in terms of a chemical reaction of Cr^{3+} oxides from the nimonic with the YBaCuO. Depth profiling of the interface region combined with AES measurements reveals also an extensive migration of nickel oxides from the substrate into the YBaCuO.

1. Introduction

One of the factors limiting the exploitation of bulk high-T_c materials is obtaining the applicable physical shape. Another is the poor mechanical stability of high-T_c materials. If the superconductor could be combined with a metallic carrier the composite would significantly improve the mechanical properties. In order to get a good adhesion between superconductor and carrier the superconductor has to be deposited in a suitable way. For this a potentially useful technique is plasma spraying which allows deposition on virtually any shape at a high deposition rate [1,2]. In previous experiments [1] the nickel-rich alloy nimonic was found to be the best substrate in terms of a higher critical temperature T_c and larger critical current density J_c. For improvement of the J_c of YBaCuO the as-deposited coatings must undergo a thermal treatment in oxygen atmosphere [1–3]. Under these conditions the interaction between substrate and YBaCuO becomes a problem, especially for longer treatments [1,4,5].

The purpose of this paper is to obtain more information concerning the interaction of a nimonic substrate with a YBaCuO layer deposited by atmospheric plasma spraying (APS). In order to get a better insight into this process we investigated the YBaCuO layer and the pure nimonic substrate. Both underwent the same thermal treatments. Auger electron spectroscopy (AES) and X-ray photoelectron spectroscopy (XPS) has been applied for the chemical characterization of these materials. The thickness and chemical composition of the interaction layer have been determined using AES in combination with the Ar^+ sputter profiling technique. In addition the substrate has also been annealed in vacuum in order to study the role of oxygen in the interaction.

2. Experimental

YBaCuO was deposited by APS on "nimonic 75" substrates with an area of $\sim 8 \times 20$ mm^2. The layers were ~ 100 μm thick. The powder used for plasma spraying consists of single-phase $YBa_2Cu_3O_x$. The high temperatures in the plasma jet melt the grains which leads to a decomposition of the $YBa_2Cu_3O_x$ phase. The de-

[1] Permanent address: Institute of Physical Chemistry, Polish Academy of Sciences, ul. Kasprzaka 44/52, 01-224 Warszawa, Poland.

composed molten grains are deposited on a "cold" substrate where they quench. Therefore, the superconducting $YBa_2Cu_3O_x$ phase has to be regrown after deposition of the layer. For this purpose the samples received the following heat treatment: 20 h at 930°C followed by 10 h at 430°C, all in 1 atm of flowing oxygen. All XPS and AES measurements were performed at room temperature on samples in the as-received state or after heat treatment.

AES measurements were performed with a PHI 600 scanning Auger microscope system. The Auger spectra and Auger sputter profiles of substrates were recorded using the following experimental conditions: primary beam energy $E_p = 10$ kV, primary beam current $I_p = 0.5$ μA and a beam diameter $\varnothing \approx 0.7$ μm. For YBaCuO we used: $E_p = 3$ kV, $I_p = 0.1$ μA and $\varnothing \approx 0.4$ μm. The resolution of the cylindrical mirror analyzer was set to 0.6%. The argon ion beam with an energy of 3.5 kV was produced by a differentially pumped ion gun. The sputter rate was calibrated using a 100 nm thick Ta_2O_5 layer. All sputter rates given in this paper are derived from this sputter rate.

The XPS experiments were carried out with a KRATOS 800 system, controlled by a PDP-11 computer. For the excitation a Mg Kα radiation source was used. The spectrometer was calibrated and its linearity checked by measuring the $Ag\,3d_{5/2}$ peak and the X-ray induced Ag MNN Auger peak on a clean sputtered silver sample. The position of the C 1s peak, relative to its normal position at 285.1 eV, was used to correct the measured binding energies (BE) for electrostatic charging of the YBaCuO sample. The spectra were taken and analyzed using a DS 800 software package. For the peak synthesis 100% Gaussians were used. Compositions for the substrates were calculated applying the empirical sensitivity factors for the pure elements [6]. For the oxides no compositions were determined as the correct sensitivity factors were not available. The absolute values for the composition may not be entirely correct due to the unknown influence of the matrix on the sensitivity factors. However, we are mainly interested in the variations in composition which can be determined very well.

The substrates were studied under three conditions: "as-received", after vacuum annealing for 20 h at 900°C with a background pressure of less than 2×10^{-7} Torr and after 20 h at 930°C in 1 atm of flowing oxygen, as used for the YBaCuO samples. The chemical composition of "nimonic 75" in weight percent is C = 0.13, Cr = 19.5, Cu $\leq$ 0.5, Ti $\leq$ 0.4, Fe $\leq$ 5.0, Si $\leq$ 1.0, Mn $\leq$ 1.0, S $\leq$ 0.02 and Ni = 62.5 [7].

In a previous study [8] we found that in situ cleaning by Ar^+ sputtering changes the chemical composition and chemical state at the surface. Because in situ scraping facilities were not available in the systems used for the present studies no surface preparation was applied.

For one sample the top 80 μm of the YBaCuO layer (with a total thickness of $\sim$ 100 μm and an area of $\sim 8 \times 20$ mm^2) spalled off. A $\sim$ 20 μm thick layer remained on the substrate. The spalling occurred after heat treatment and is probably due to strains caused by the chemical interaction with the substrate. The YBaCuO layer separated in the reacted region, which gave us the opportunity to study the reaction products by both AES and XPS.

3. Results

3.1. AES / XPS analysis of the YBaCuO / nimonic interface region

Fig. 1 shows the Auger spectrum of the surface obtained after the top of the YBaCuO layer spalled off. It reveals Cr in addition to Ba, Cu, Y, O and C. No nickel was detected.

Auger depth profiles of the interacted region are measured for O KLL, Cu LMM, Ba MNN, Ni LMM and Cr LMM. Yttrium was not measured because its low sensitivity factor would have increased the measurement time to much. The scaled peak-to-peak (PTP) heights have been plotted as a function of sputter time in fig. 2. The sputter rate was $\sim$ 43 nm/min. The sputter profile presented here is the only one where we succeeded to measure the interface with the substrate. Due to the rough interface between substrate and plasma sprayed layer other attempts

did not succeed in reaching the interface within the duration of the experiment. The general behavior in the reacted region is similar in all the measured spots. Also the trend shown in fig. 2 is supported by SEM/EDX analysis on cross-sections of similar samples.

Chromium is found through the whole reacted YBaCuO region, whereas nickel appears first after 60 min of sputtering. This shows that the transport of Cr in YBaCuO is faster than that of nickel. The noise in the PTP heights as a function of sputter time can be caused by a porous structure of the YBaCuO or is due to a variation in the stoichiometry of the bulk YBaCuO deposit. Probably both effects play a role, since the YBaCuO decomposes during deposition and SEM analysis shows the presence of micro-cracks in this type of samples. In fig. 2 we see that the concentration of Ba decreases systematically compared to that of Cu, Ni, O and Cr after ~ 300 min of sputtering.

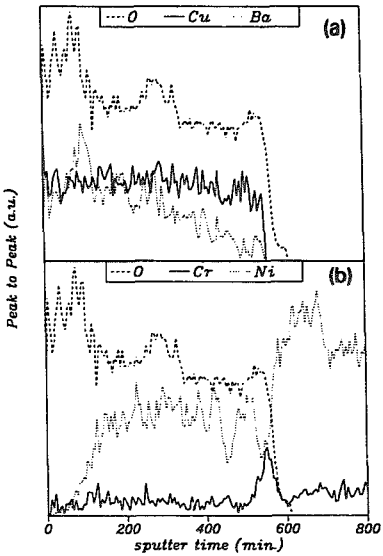

Fig. 2. Auger sputter profile of interacted region between YBaCuO and substrate measured after spalling for the elements Cu and Ba (a) and Cr and Ni (b). The sputter profile for oxygen is shown in both (a) and (b). The sputter rate was 43 nm/min.

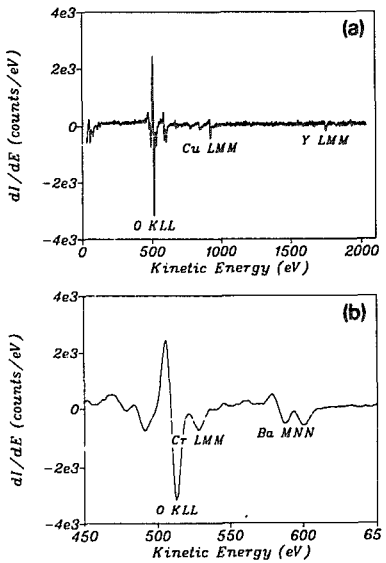

Fig. 1. (a) Auger spectrum of YBaCuO reacted with the nimonic substrate (see also text). (b) Detail of (a).

The presence of Cr on the surface of the reacted YBaCuO was confirmed by XPS investigations. In order to discuss the chemical nature of the Cr compounds present we measured the Cr 2p XPS spectra on the reacted YBaCuO (line 1) and the nimonic substrate for various heat treatments (lines 2, 3, 4), as shown in fig. 3.

In reacted YBaCuO the major Cr 2p peak is found at 579.8 eV. This is typical for Cr^{6+}, suggesting the presence of $BaCrO_4$ [10]. The "as-received" and in oxygen annealed substrates (lines 2 and 3 respectively) are characterized by a main Cr 2p peak at 576.5 eV, which is typical for Cr^{3+} and Cr^{4+} and can be attributed to the presence of Cr_2O_3 [11,12] and CrO_2 [13]. The broadening on the low energy side of the Cr 2p peak of the "as-received" substrate indicates the presence of metallic Cr. The Cr 2p peak of the vacuum annealed substrate (line 4) is positioned at 574.1

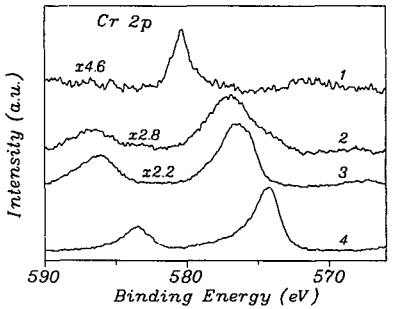

Fig. 3. Cr2p XPS spectra taken from reacted YBaCuO (line 1) and the nimonic substrate: "as-received" (line 2), after annealing at 930°C in oxygen atmosphere (line 3) and after annealing at 900°C in high vacuum (line 4).

eV, typical for the presence of metallic chromium [14]. A detailed peak-synthesis analysis of the Cr 2p spectra is not possible because of the overlap with induced Ba MNN and Ni LMM Auger peaks.

The above interpretation is supported by analysis of the O 1s spectra of the "reacted" and "unreacted" YBaCuO. Reacted YBaCuO is, as before, material that has reacted with the substrate during heat treatment. Unreacted YBaCuO is material that has not reacted with the substrate during the heat treatment. The O 1s spectra of reacted (line 1) and unreacted (line 2) YBaCuO are shown in fig. 4. The two peaks at ~ 531.5 and ~ 528.9 eV are found in both spectra and are usually attributed to oxygen on the surface and in the bulk of the YBaCuO, respectively [15,16]. Apart from the previous two peaks the spectrum of reacted YBaCuO shows a peak at 530.3 eV. This additional state can be attributed to oxygen in oxides like $BaCrO_4$ or CrO_3 [17].

3.2. AES / XPS investigations of nimonic

The influence of different heat treatments on the Ni 2p XPS spectrum of the nimonic substrates is shown in fig. 5. After annealing at 900°C for 20 h in high vacuum, only the characteristic spectrum of pure Ni [14] with the main peak at 852.8 eV is found (line 3). This agrees well with the

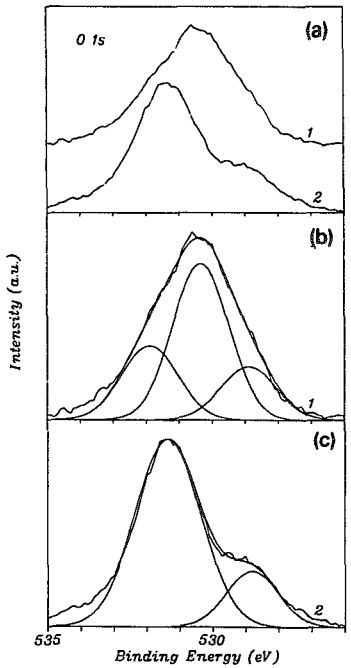

Fig. 4. (a) O 1s XPS spectra of the reacted (line 1) and unreacted (line 2) YBaCuO. For explanation see text. (b,c) Deconvolution of the spectra in (a).

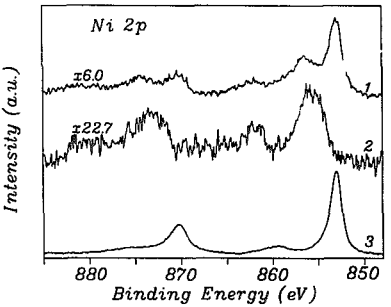

Fig. 5. Ni2p XPS spectra of nimonic "as-received" (line 1), after annealing in oxygen atmosphere at 930°C (line 2) and after annealing in high vacuum at 900°C (line 3).

spectra reported for Ni–Cr alloys [18]. Annealing in oxygen at high temperature results in an increased intensity of the doublet as compared to the main peak (line 2). In this case the main peak lies at 855.9 eV, which corresponds to Ni^{3+}, possibly present in the form of Ni_2O_3 [19]. Both the oxidized and pure nickel states are found for substrates in the "as-received" state (line 1). However, in this case the Ni 2p peak at 856.5 eV can also be interpreted in terms of the presence of hydroxyl groups [19] as a result of adsorption of H_2O on the surface.

Apart from Ni and Cr other elements are also detected. The results of a quantitative evaluation of their concentrations, performed by XPS and AES, are presented in table 1.

XPS analysis of the substrate after annealing in high vacuum showed the presence of a significant amount of Ti, S and C, but no oxygen. In the AES measurement oxygen was found on the same sample. This is because the sample was annealed in situ in the XPS vacuum system and was then transported through air to the AES vacuum system. The XPS spectrum of Ti 2p shows a doublet with the major peak at 454.8 eV, which can be attributed to TiC [14]. This is confirmed by the analysis of the C 1s spectrum. The analysis allows us to distinguish at least 3 peaks at 282.0, 282.8 and 284.0 eV, which can be identified as the carbides of Ti [20], Cr [21] and Ni [22], respectively. A relatively high concentration of sulphur was found (see table 1). The S 2p spectrum has a peak at 161.7 eV, which suggest a sulphide character of the S state [14,23]. This tendency of Ti, C and S to segregate and the formation of TiC at the surface is also found in FeAlTi alloys [24].

The enrichment of C and S is restricted to the surface region ($\leq$ 10 nm thick), as was shown by Auger depth profile measurements (see also table 1). Both the "as-received" and vacuum annealed samples show a homogeneous bulk depth distribution of elements after 2–3 min of sputtering (corresponding to a depth of $\sim$ 10 nm).

Annealing of the nimonic substrates for 20 h at 930°C in oxygen atmosphere changes significantly the surface composition (table 1). XPS and AES spectra have been recorded at room temperature in the as-received state or after heat treatment. Apart from the oxidized states of Ni (fig. 5) and Cr (fig. 3), we observe a relative abundance of Ti and Mn oxides. The main peaks of Ti 2p (458.5 eV) and Mn 2p (641.5 eV) agree well with those reported for TiO_2 and MnO [14]. This is confirmed by an analysis of the corresponding O 1s spectra shown in fig. 6. Deconvolution of the O 1s spectra shows the presence of three peaks. The main peak at 530.0 eV can be attributed to the following oxides: Cr_2O_3, TiO_2, MnO [25] and

Table 1
Ni, Cr, O, C, Ti, Mn, Fe and S concentration at the surface of nimonic substrates after different heat treatments

Heat treatment	Analysis method	Atomic concentration (%)							
		Ni	Cr	O	C	Ti	Mn	Fe	S
"as-received"	XPS	10.6	10.3	38.6	39.4	0.4	–	0.8	–
	AES	30.7	8.5	27.5	33.1	< 1.0	–	< 1.0	–
	*	72.0	15.9	2.2	8.3	< 1.0	–	< 1.0	–
Heating in vacuum (900°C)	XPS	47.9	25.3	–	14.5	2.7	–	1.4	8.2
	AES	31.6	13.9	7.8	32.6	4.9	–	< 1.0	9.0
	*	69.0	16.5	–	8.5	5.0	–	< 1.0	–
Heating in oxygen (930°C)	XPS	3.5	10.2	53.8	23.1	2.5	6.8	–	–
	AES	5.5	4.6	44.7	27.0	10.9	7.2	–	–
	*	9.8	8.9	56.3	7.1	9.3	8.6	–	–

The second entries for the AES results, denoted with an asterisk (*), have been measured after removing a layer of $\sim$ 10 nm by argon ion sputtering. The first entries for the AES results are the values found before sputtering. The composition for the "as-received" substrate after sputtering and the vacuum annealed substrate show nickel and chromium compositions comparable to literature data [7].

NiO [19]. The peak at 531.6 eV fits well with the Ni_2O_3 state [14], whereas the peak at ~ 533.0 eV can be attributed to adsorption of molecular oxygen [26]. The ratio of the oxygen peak areas at 530.0 and 531.6 eV is much larger for the oxidized than for the "as-received" sample, indicating an increased concentration of the oxides of Cr (and also Ti and Mn) at the surface due to the high temperature oxidation.

The depth distribution of elements after heat treatment in oxygen has been determined at room temperature by measuring the Auger sputter profiles. The results are presented in fig. 7. The peak-to-peak heights of the O KLL, Cr LMM, Ni LMM, Mn LMM and Ti LMM Auger peaks have been plotted as a function of sputter time. Some characteristic points can be distinguished in the profile. After sputtering for ~ 10 min a small maximum is found in the concentration of Mn, Ti and Ni, accompanied by a minimum in the concentration of O. Further sputtering results in an increase of the Cr and O and a decrease of the Mn, Ti and Ni concentrations. After the maximum in O and Cr concentrations at ~ 30 min we observe a continuous decrease of the O and Cr and increase of Ni concentration, whereas the amount of Ti and Mn remains constant.

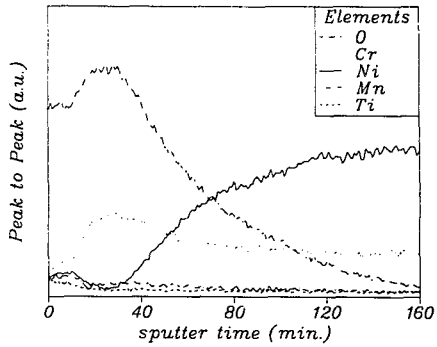

Fig. 7. Auger sputter profiles of nimonic after annealing in oxygen at 930°C. The sputter rate was 4.3 nm/min for the first 10 min and 43 nm/min for the rest of the time.

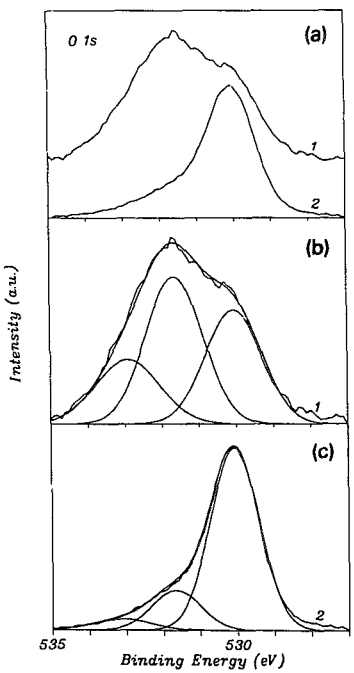

Fig. 6. (a) O 1s XPS spectra of nimonic: "as-received" (line 1) and after annealing in oxygen at 930°C (line 2). (b,c) Deconvolution of the spectra in (a).

Using the sputter rate indicated in the caption of fig. 7 the thickness of the layer enriched in Mn and Ti oxides is estimated to be ~ 0.4 μm. A significant abundance of Cr is found at a depth of more than 0.1 μm with a maximum at ~ 0.9 μm.

4. Discussion

The presented results show an extensive interaction between the nimonic and YBaCuO. Both the duration and temperature seem to be important in the process. Tachikawa et al. [1] did not observe a considerable diffusion of Ni into plasma sprayed YBaCuO after annealing for 1 h at 900°C. In our case the samples were annealed in oxygen for 20 h at 930°C. In this period of time and at this temperature both the diffusion of oxygen through the polycrystalline YBaCuO layer and the interaction of the YBaCuO with the substrate will be more extensive.

A significant segregation of sulphur, carbon and titanium was observed for nimonic annealed under high vacuum conditions. The first two elements are known to segregate to alloy grain boundaries during heat treatment [29,30]. Segregation of Ti can be explained in terms of the Miedema theory [31], as Ti has a lower surface enthalpy compared to Ni and Cr. The tendency of segregation of Ti, C and S to the surface is also found in FeAlTi alloys [24], although here the details of the mechanisms involved might be different.

Annealing in oxygen atmosphere induces segregation of Ti, Ni and Cr at the surface of the substrate. The segregation is much stronger than for the vacuum annealed sample because oxidation of the elements at the oxide/metal interface leads to the formation of phases which are thermodynamically more stable. The mechanism of that process has been studied earlier for Ni–Cr alloys [32,33]. Because of the larger oxygen affinity, chromium in the alloy is preferentially oxidized according to the reaction [32]

$$3\ NiO + 2\ Cr \rightarrow Cr_2O_3 + 3\ Ni, \qquad (1)$$

promoting the formation of a Cr_2O_3 phase in the surface region and a thin NiO layer concentrated at the outermost surface. The results shown in figs. 2 and 7 fit well with this mechanism. In both figures the Cr_2O_3 enrichment at the surface of the substrate is present. This shows that the segregation in the substrate covered with YBaCuO is also influenced by oxygen.

At temperatures above 800°C, nickel oxide can form coexisting phases with barium oxide [34]. The specific composition formed depends on the extent of nickel oxide migration. In the range over which a decrease in Ba concentration is observed (from ~ 300 min of sputtering up to the interface) nickel is found. Also in the region where the Ba concentration becomes constant the nickel concentration goes to zero. Since in the as-deposited layer the barium concentration is expected to be more or less homogeneous, this suggests Ba transport has taken place as a result of the in-diffusion of nickel oxide. This is supported by the constant concentration profile found for Cu (see fig. 2a).

The nature of chromium interaction with YBaCuO is more complex. The chromium contents appears to be more or less constant in the reacted layer, which is not expected for a diffusion type of transport. Identification of Cr^{6+} state in reacted YBaCuO (fig. 3) suggests a chemical reaction of chromium oxide with the deposit. The Cr and Ni oxide phases can form nickel and barium chromites ($NiO \cdot Cr_2O_3$, $BaO \cdot 4Cr_2O_3$). Further oxidation then results in a rearrangement of the three-valent chromite state into six-valent chromate compounds by one of the following reactions:

$$\begin{aligned} &4\ NiO \cdot Cr_2O_3 + 8\ BaO + 7\ O_2 \\ &\quad \rightarrow 2\ Ni_2O_3 + 8\ BaCrO_4, \\ &3\ NiO + 2\ BaO + Cr_2O_3 \rightarrow 2\ BaCrO_4 + 3\ Ni, \\ &2\ Cr_2O_3 + 4\ BaO + O_2 \rightarrow 4\ BaCrO_4. \end{aligned} \qquad (2)$$

Each of the above reactions requires an equivalent amount of chromium and barium oxide. Only the necessary amounts of nickel oxide and free oxygen are different. This means that the formation of $BaCrO_4$ can also take place in the absence of free oxygen. The above might have explained the constant chromium concentration if also the barium contents had been constant in the reacted layer. Since the barium concentration decreases towards the interface, the formation of $BaCrO_4$ can only be part of the whole process. As barium can form compounds with most of the other metal-oxides present in the substrate and YBaCuO, the situation is very complex. The information available at this moment is insufficient to discriminate between the different reaction mechanisms.

The elements C, S, Ti and Mn, present at the surface of annealed nimonic, were not detected in the reacted YBaCuO. This is not surprising as, in this case, these elements are not pinned at the surface of the substrate but can diffuse into the YBaCuO. As a result the concentration of these elements decreases below the detection limit.

5. Conclusions

Prolonged high temperature annealing of plasma sprayed YBaCuO deposited on nimonic

substrates results in an extensive interaction with the substrate. Nickel oxide compounds migrate into the YBaCuO layer. Also migration of Ba seems to take place. Cr^{3+} compounds from the substrate react with YBaCuO and free oxygen to form six-valent chromate compounds. The presence of oxygen plays an important role in the surface segregation of Cr and the trace elements Ti and Mn from the nimonic substrate. The oxygen needed for this process appears to be both available from free oxygen diffusing along the grain boundaries and reactions with the YBaCuO (as shown in eq. (2)). This suggests that a change in annealing atmosphere will not stop the interaction between nimonic and YBaCuO. In order to check the role of the annealing atmosphere it would be necessary to study the interaction between substrate and YBaCuO in gases like Ar, He, N_2 and NO.

Acknowledgements

This work was supported by the Commission of the European Community within the Brite–EuRam program under contract BREU-0124.

References

[1] K. Tachikawa, I. Watanabe, S. Kosuge, M. Kabasawa, T. Suzuki, Y. Matsuda and Y. Shinbo, Appl. Phys. Lett. 52 (1988) 1011.
[2] J. Lacombe, J. Danroc and G. Kurka, J. Less-Common Met. 164/165 (1990) 509.
[3] S. Jin, T.H. Tiefel, R.C. Sherwood, R.B. van Dover, M.E. Davis, G.W. Kammlott and R.A. Fastnacht, Phys. Rev. B 37 (1988) 7850.
[4] W.A.M. Aarnink, D.H.A. Blank, D.J. Adelerhof, J. Flokstra, H. Rogalla and A. van Silfhout, Appl. Surf. Sci. 47 (1991) 195.
[5] C.T. Cheung and E. Ruckenstein, J. Mater. Res. 4 (1989) 1.
[6] D. Briggs and M.P. Seah, Practical Surface Analysis by Auger and X-Ray Photoelectron Spectroscopy (Wiley, Chichester, 1983).
[7] C.W. Wegst, Stahlschlüssel, Verlag Stahlschlüssel Wegst K.G. (1977).
[8] W. Lisowski, H. Hemmes, D. Jäger, A. van Silfhout, D. Stöver and L.J.M. van de Klundert, in: High Temperature Superconductor Thin Films, Proc. Symp. A1 Int. Conf. on Advanced Materials 1991 (ICAM91), 27–31 May 1991, Strasbourg, France, Ed. L. Correra (North-Holland, Amsterdam, 1992) p. 683.
[9] L.E. Davis, N.C. MacDonald, P.W. Palmberg, G.E. Riach and R.E. Weber, Handbook of Auger Electron Spectroscopy (Perkin-Elmer, Physical Electronics Division, Eden Prairie, MN, 1978).
[10] G.C. Allen and P.M. Tucker, Inorg. Chim. Acta 16 (1976) 41.
[11] C. Battistoni, J.L. Dorman, D. Fiorani, E. Paparazzo and S. Viticoli, Solid State Commun. 39 (1981) 581.
[12] G.C. Allen, P.M. Tucker and R.K. Wild, J. Chem. Soc. Faraday Trans. II, 74 (1978) 1126.
[13] I. Ikemoto, K. Ishii, S. Kinoshita, H. Kuroda, M.A.A. Franco and J.M. Thomas, J. Solid State Chem. 17 (1976) 425.
[14] C.D. Wagner, W.M. Riggs, L.E. Davis and J.F. Moulder, Handbook of X-Ray Photoelectron Spectroscopy (Perkin-Elmer, Physical Electronics Division, Eden Prairie, MN, 1979).
[15] S.L.T. Andersson and J.C. Otamiri, Appl. Surf. Sci. 45 (1990) 1.
[16] W.A.M. Aarnink, J. Gao, H. Rogalla and A. van Silfhout, J. Less-Common. Met. 164/165 (1990) 321.
[17] T. Dickinson, A.F. Povey and P.M.A. Sherwood, J. Chem. Soc. Faraday Trans. I, 72 (1976) 686.
[18] F.V. Hillebrecht, J.C. Fuggle, P.A. Bennett and Z. Zolnierek, Phys. Rev. B 27 (1982) 2179.
[19] K.S. Kim and N. Winograd, Surf. Sci. 43 (1974) 625.
[20] H. Ihara, Y. Kumashiro, A. Itoh and K. Maeda, Jpn. J. Appl. Phys. 12 (1973) 1462.
[21] L. Ramqvist, K. Hamrin, G. Johansson, A. Fahlman and C. Nordling, J. Phys. Chem. Solids 30 (1969) 1835.
[22] S. Sinharoy and L.L. Levenson, Thin Solid Films 53 (1978) 31.
[23] H. van der Heide, R. Hemmel, C.F. van Bruggen and C. Haas, J. Solid State Chem. 33 (1980) 17.
[24] H. Viefhaus, J. Peters and H.J. Grabke, Surf. Interf. Anal. 10 (1987) 280.
[25] C.D. Wagner, D.A. Zatko and R.H. Raymond, Anal. Chem. 52 (1980) 1445.
[26] C.R. Brundle, Surf. Sci. 48 (1975) 99.
[27] G. Gillen, D.L. Kaiser and J.S. Wallace, Surf. Interf. Anal. 17 (1991) 7.
[28] S.J. Rothman, J.L. Rontbort and J.E. Baker, Phys. Rev. B 40 (1989) 8852.
[29] J. Küpper, H.J. Grabke and H. Viefhaus, Surf. Interf. Anal. 12 (1988) 223.
[30] P. Marcus, A. Elbiache and H. Chadli, Appl. Surf. Sci. 27 (1986) 71.
[31] J.R. Chelikowsky, Surf. Sci. 139(1984) L197.
[32] N.S. McIntyre, D.G. Zetaruk and D. Owen, Appl. Surf. Sci. 2 (1978) 55.
[33] J. Steffen and S. Hofmann, Surf. Interf. Anal. 11 (1988) 617.
[34] M. Levin, C.R. Rabbins and H.F. McMurdie, Phase Diagrams for Ceramics (The American Ceramic Society, Columbus, OH, 1964).